

# Refraction of finite-amplitude water waves: deep-water waves approaching circular caustics

By D. H. PEREGRINE

School of Mathematics, University of Bristol

(Received 22 September 1980)

The ‘numerically exact’ properties of plane periodic deep-water waves are used in a slowly-varying-wave approximation for a steady axisymmetric wave field. The linear ‘ray’ theory for such a wave field corresponds to waves approaching a circular caustic. A parameter,  $C$ , characterizes each solution. If  $C$  is smaller than 20 the wave behaviour is dominated by the convergence of wave energy and waves are expected to break. Comparison with experiment for  $C = 0$  indicates that breaking may be accurately predicted. If  $C$  is greater than 50 then the waves propagate closer to the caustic and, since it is of Peregrine & Smith’s (1979) type R, it is likely that the waves do not break. These solutions show that wave action does not flow along the straight lines of the linear rays.

---

## 1. Introduction

‘Numerically exact’ solutions for properties of plane periodic water waves (Longuet-Higgins 1975; Cokelet 1977) make it possible to investigate the refraction of finite-amplitude water waves. It is still necessary to make the relatively severe approximation that on the scale of individual waves the wave field has all the properties of a plane periodic train of waves.

The refraction of deep-water waves by two simple current distributions is dealt with by Peregrine & Thomas (1979) which is referred to hereafter as I. The behaviour of the solution near two types of caustic is investigated there. More general analysis, but limited to near-linear waves, in Peregrine & Smith (1979) shows that near-linear caustics come in two varieties which they label R and S, corresponding to ‘regular’ and ‘singular’. It seems, but is not proved, that the breaking of water waves due to the proximity of a caustic is only likely for S type caustics. As noted by Peregrine & Smith all water wave caustics on still water are of the R type.

Study of the refraction of finite-amplitude water waves in finite depth of water has followed. Stiassnie & Peregrine (1979) derive relevant averaged equations following Phillips (1966), Whitham (1974) and Crapper (1979). The effects of depth variation for the case of parallel depth contours and a single incident plane wave are treated for normally incident waves by Stiassnie & Peregrine (1980) and for obliquely incident waves by Ryrie & Peregrine (1981). This later paper includes the case of depth-induced caustics which are very similar to the R type caustics of I despite the fact that extra ‘potential’ variables, viz. the depth and current, not considered by Peregrine & Smith (1979) are involved.

The present study of waves approaching a circular caustic uses the same approach as I. It is clear from Peregrine & Smith (1979) that a circular caustic is of R type for water waves, at least insofar as near-linear theory is applicable. However, unlike the R type caustics of I and Ryrie & Peregrine (1981), the convergence of wave energy can lead to wave breaking before the vicinity of the caustic is reached. This is particularly so in the limit where the radius of the circle tends to zero and waves approach the centre with crests in the form of contracting circles. For this particular case comparison with experiment is possible. A sector of the circle corresponds to waves propagating into a converging wedge-shaped channel. Such waves have been measured by van Dorn & Pazan (1975) and the measurements show that the finite-amplitude results are an improvement over linear theory. The experimental results include observations on the breaking of waves. The finite-amplitude theory, together with Longuet-Higgins's (1978) result for rapid instability of waves greater than a critical steepness, appear to give a good guide to the onset of breaking.

There is a simple discussion of the corresponding linear theory in order to provide a framework for discussion of the later results and since some of the analysis is identical for the finite-amplitude waves. After the mathematical theory is briefly presented two special cases are discussed: (i) an exact focus, that is the example with circular crests mentioned above, and (ii) radial waves, that is with crests like the spokes of a wheel. These are limiting cases,  $C = 0$  and  $C = \infty$ , for a dimensionless caustic parameter which characterizes the whole family of solutions. Infinitesimal waves also correspond to  $C = \infty$  and there are two branches of the solution for all sufficiently large  $C$ . Typical examples for intermediate values of  $C$  are presented.

These examples show that the wave energy does not always propagate in straight lines despite the fact that the medium is homogeneous and isotropic. This is not entirely surprising in view of past work on nonlinear wave propagation. For deep-water waves the propagation velocities of small modulations are the group velocity, twice, for linear waves, but are complex for finite-amplitude waves (see Hayes 1973; Whitham 1974; or I). This divergence from straight lines corresponds to the self-focusing (or de-focusing) discussed in Whitham (1974, §16.3) for a different geometry.

## 2. Linear theory

For infinitesimal waves of frequency  $\sigma$  on deep water the velocity potential can be written

$$\phi(\mathbf{r}) e^{-kz - i\sigma t}, \quad (2.1)$$

where  $k = \sigma^2/g$ ,  $z$  is vertically upwards, and  $\mathbf{r}$ , like other vectors in this paper, is a two-dimensional horizontal vector. The function  $\phi(r)$  satisfies Helmholtz's equation

$$\nabla^2 \phi + k^2 \phi = 0, \quad (2.2)$$

for which exact solutions in polar co-ordinates,  $(r, \theta)$ , are the Bessel function solution

$$J_n(kr) e^{in\theta}, \quad (2.3)$$

and the Hankel function solution

$$H_n^{(1)}(kr) e^{in\theta}. \quad (2.4)$$

The Bessel function solution (2.3) is regular everywhere and corresponds to waves meeting a circular caustic in the neighbourhood of  $r = n/k$  and then proceeding to propagate away from it. The number of waves around the caustic is  $n$ . The Hankel

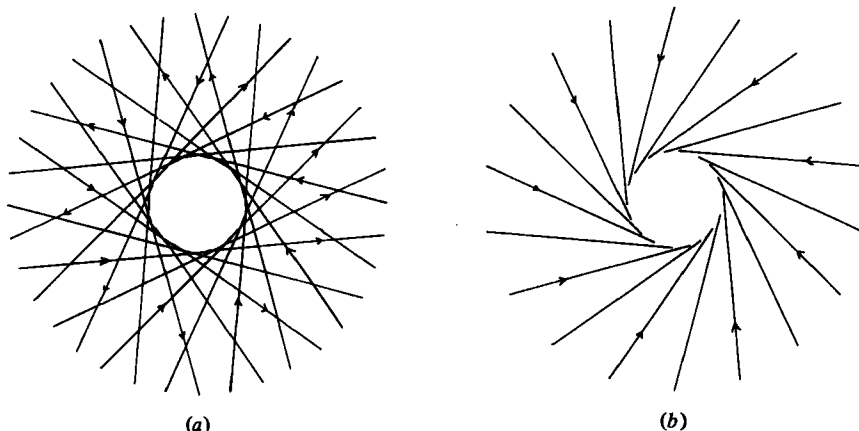


FIGURE 1. (a) The rays of the Bessel function solution (2.3).  
 (b) The rays of the Hankel function solution (2.4).

function solution (2.4) corresponds only to waves coming towards the caustic and within the caustic circle its modulus increases towards a singularity at the origin. This latter solution (or the  $H_n^{(2)}$  function for waves receding from a caustic) is the exact linear solution corresponding to the nonlinear solutions which follow.

A more intuitive version of these two solutions is given by their 'ray' descriptions which are portrayed in figure 1. This description amounts to treating the waves as if they are locally plane waves. It is helpful to do this first for the linear case where comparison can be made with the exact solutions.

Consider one ray, as in figure 2. If the angle between the ray and a radial line to the origin is  $\alpha$  then the wavenumber may be written as

$$\mathbf{k} = -k \cos \alpha \hat{\mathbf{r}} + k \sin \alpha \hat{\boldsymbol{\theta}}, \quad (2.5)$$

where  $\hat{\mathbf{r}}$  and  $\hat{\boldsymbol{\theta}}$  are unit vectors in the co-ordinate directions. The wave field is assumed to be described by an expression

$$ae^{i\chi}, \quad (2.6)$$

where

$$\mathbf{k} = \nabla \chi. \quad (2.7)$$

On a large scale  $a$  and  $\alpha$  are assumed to vary with position. For a steady axisymmetric wave field this means they are functions of  $r$  alone. However, for (2.7) to be a consistent expression we must have

$$\nabla \times \mathbf{k} = 0 \quad (2.8)$$

everywhere and this reduces to

$$\frac{\partial}{\partial r}(r\mathbf{k} \cdot \hat{\boldsymbol{\theta}}) = 0,$$

since  $k$  is independent of  $\theta$ . Integration gives

$$rk \sin \alpha = n, \quad (2.9)$$

where the constant of integration has been put equal to  $n$  by comparison with the exact solution (e.g. when  $\alpha = \frac{1}{2}\pi$ ). From (2.9) we immediately have

$$k \cos \alpha = (k^2 - n^2/r^2)^{\frac{1}{2}}, \quad (2.10)$$

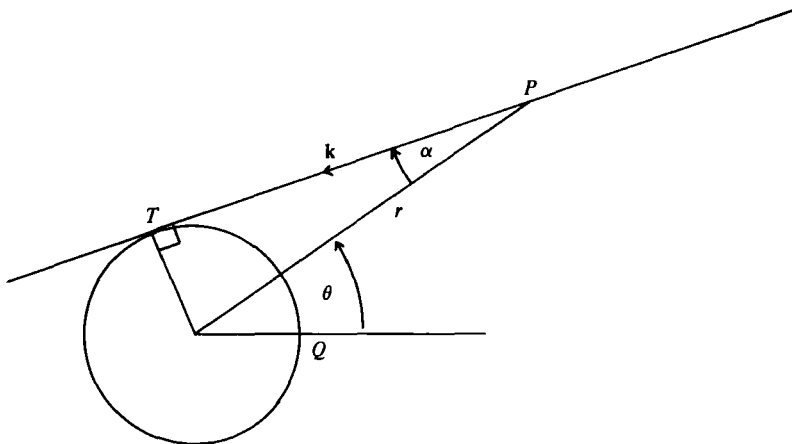


FIGURE 2. Definition diagram for a ray.

and can then integrate equation (2.7) to give

$$\chi = -(k^2 r^2 - n^2)^{\frac{1}{2}} + n \cos^{-1}(n/kr) + n\theta \quad (2.11)$$

within a constant.

The expression for  $\chi$  can be developed in a different way by considering phase directly. Suppose phase is referred to a reference point at  $Q$ , see figure 2. On the caustic circle at  $r = n/k$ , which has  $n$  waves around it, the phase at  $T$  is  $(\theta + \frac{1}{2}\pi - \alpha)n$ . The distance  $TP$  is  $(r^2 - n^2/k^2)^{\frac{1}{2}}$  so the difference in phase between  $T$  and  $P$  is  $-(k^2 r^2 - n^2)^{\frac{1}{2}}$ . Adding these together and noting  $\cos(\frac{1}{2}\pi - \alpha) = n/kr$  gives the expression (2.11) again for the phase at  $P$ . This time the integration constant is defined by the reference to  $Q$ .

The wave amplitude comes from the conservation of wave action. For this steady problem, this gives

$$\nabla \cdot \mathbf{B} = 0, \quad (2.12)$$

where  $\mathbf{B}$  is the wave-action flux, or by the radial symmetry

$$\frac{1}{r} \frac{\partial}{\partial r} (r \mathbf{B} \cdot \hat{\mathbf{r}}) = 0. \quad (2.13)$$

Now, the wave-action flux is in the  $\mathbf{k}$  direction, so, with  $|\mathbf{B}| = B$ , equation (2.13) integrates to

$$rB \cos \alpha = \text{constant}. \quad (2.14)$$

For linear waves the wave-action flux is  $\frac{1}{4}\rho g a^2/k$ ; thus

$$a = a_1 (r \cos \alpha)^{-\frac{1}{2}} = a_1 (r^2 - n^2/k^2)^{-\frac{1}{4}}, \quad (2.15)$$

where  $a_1$  is a constant. This result is also readily derived from figure 2 by noting that 'adjacent' rays meet at the caustic and  $B$  is therefore inversely proportional to the length  $TP$ .

The results (2.11) and (2.15) substituted in (2.6) indicate that an approximation to  $H_n^{(1)}(kr)$  is

$$a_1 (r^2 - n^2/k^2)^{-\frac{1}{4}} \exp i[-(k^2 r^2 - n^2)^{\frac{1}{2}} + n \cos^{-1}(n/kr)], \quad (2.16)$$

or

$$a_1 (r \cos \alpha)^{-\frac{1}{2}} \exp i[-kr \cos \alpha + n(\frac{1}{2}\pi - \alpha)]. \quad (2.17)$$

This is indeed an asymptotic expansion of  $H_n^{(1)}$  for large  $n$ ; the corresponding results for  $J_n$  and  $Y_n$  are given in Abramowitz & Stegun (1964), §9.3.3, with  $\beta = \frac{1}{2}\pi - \alpha$ .

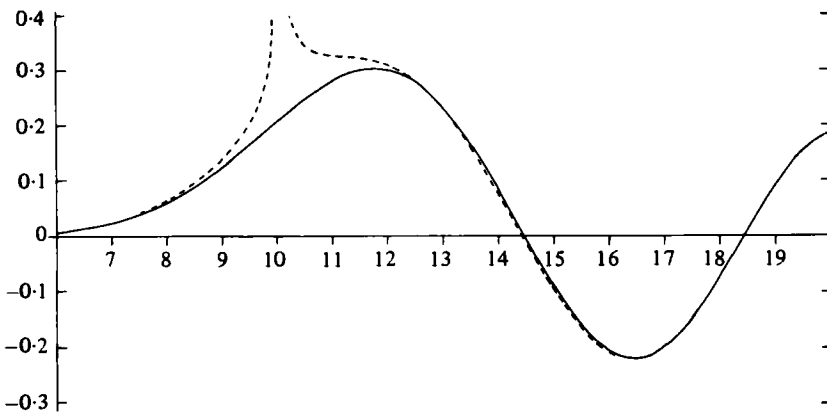


FIGURE 3. A comparison of  $J_{10}(z)$ , full line, with its asymptotic expansions, broken line.

A comparison between  $J_{10}(z)$  and the asymptotic expansion corresponding to (2.16) with the appropriate constant multiplier is given in figure 3. The asymptotic expansion for  $z < 10$ , which needs little modification of (2.16), is also given. As so often happens, the approximation is remarkably good.

### 3. Finite-amplitude theory

For finite-amplitude waves the wavenumber is not constant for a given frequency but varies with wave steepness. The dispersion equation may be written

$$\sigma^2 = gkS(s), \quad (3.1)$$

where  $s = a^2k^2$  is the steepness squared. The notation follows I.

The kinematic relationships involving  $\mathbf{k}$  are no different from those of linear theory so that equations (2.9) and (2.10) still hold. However, direct integration to a phase function as in (2.11) is not possible since  $k$  is not constant, but an unknown function of  $r$ .

Wave-action flux is conserved and again the derivation for linear theory holds up to equation (2.14). However,  $B$  is a more complicated function. Using equation (2.13) of I we write (2.14) in the form

$$(\rho g/2k^3)(E + 5L)r \cos \alpha = \rho gb, \quad (3.2)$$

where  $b$  is a constant and  $E(s)$  and  $L(s)$  are dimensionless measures of the energy density and averaged Lagrangian, defined in I.

Once  $\sigma$ ,  $n$  and  $b$  are given, the unknown functions of  $r$  are  $k$ ,  $\alpha$  and  $s$ . If a value of  $s$  is chosen equation (3.1) gives  $k$ ; then equations (2.9) and (3.2) can be solved for  $r$  and  $\alpha$ . That is,  $r$ ,  $k$  and  $\alpha$  are given as functions of  $s$  by

$$k = \sigma^2/gS, \quad (3.3)$$

$$r = \frac{ngS}{\sigma^2} \left[ 1 + \frac{4\sigma^{16}b^2}{g^8n^2S^8(E+5L)^2} \right]^{\frac{1}{2}}, \quad (3.4)$$

$$\tan \alpha = \frac{g^4nS^4(E+5L)}{2\sigma^8b}. \quad (3.5)$$

It can be seen from equation (3.4) that an appropriate dimensionless radius is

$$R = \sigma^2 r / ng \quad (3.6)$$

and similarly

$$K = gk / \sigma^2 \quad (3.7)$$

for the wavenumber. At a linear caustic  $R = 1$  and  $K = 1$ . The above solutions depend on the single dimensionless constant

$$C = g^4 n / \sigma^6 b, \quad (3.8)$$

$C$  for 'caustic parameter'. An alternative expression is

$$C = g^3 r_c / \sigma^6 b, \quad (3.9)$$

where  $r_c$  is the radius of the linear caustic. First we consider the cases  $C = 0$  and  $C = \infty$ .

#### 4. The perfect focus

For the case of waves travelling directly towards the origin  $n = 0$ ,  $\alpha = 0$  and equation (3.2) can be written as

$$S^3 (E + 5L)r = 2\sigma^6 b / g^3, \quad (4.1)$$

which is a single equation between  $r$  and  $s$ . It is shown, with slightly different variables, in figure 4.

One realization of this configuration is obtained when waves propagate on deep water between converging walls. This gives a sector from the complete circular waves the solution can describe. However, it is also a realistic experimental configuration which has been used by van Dorn & Pazan (1975) who give tables of measurements of waves in a channel with a 1:10 convergence. In particular, they give measurements of wave steepness,  $H/L = ak/\pi$ , and channel width,  $w$ , for different wave frequencies and different amplitudes of wavemaker displacement.

The main aim of van Dorn & Pazan's work was to study wave breaking so that only some of their measurements are suitable for comparison with equation (4.1). Data for one wave train has been considered usable if there are a minimum of six measurements of the wave train before its amplitude is reduced by breaking. Six sets of data satisfy this criterion and all are included here. Points which are identified as breaking waves, or as waves that have broken are included only if their steepness is greater than the steepness at the previous measuring point.

In order that a data set can be compared with (4.1), or the equivalent linear-theory equation, it is necessary to use some of the data to determine the constant  $b$ . In an initial plot of the data the first measurement was used; however, on consideration it seems more appropriate to use the average value from the whole data set. Thus for every point the quantity

$$b_1 = S^3 (E + 5L)w, \quad (4.2)$$

which is proportional to  $b$  in equation (4.1), and

$$b_0 = \frac{1}{2} \alpha^2 k^2 w, \quad (4.3)$$

which is the corresponding linear-theory quantity, were calculated. Cokelet's (1977) tables were used. The mean values of  $b_0$  and  $b_1$  are given in table 1. Of course, when all the points are plotted, as they are in figure 4, this does mean that the theoretical line

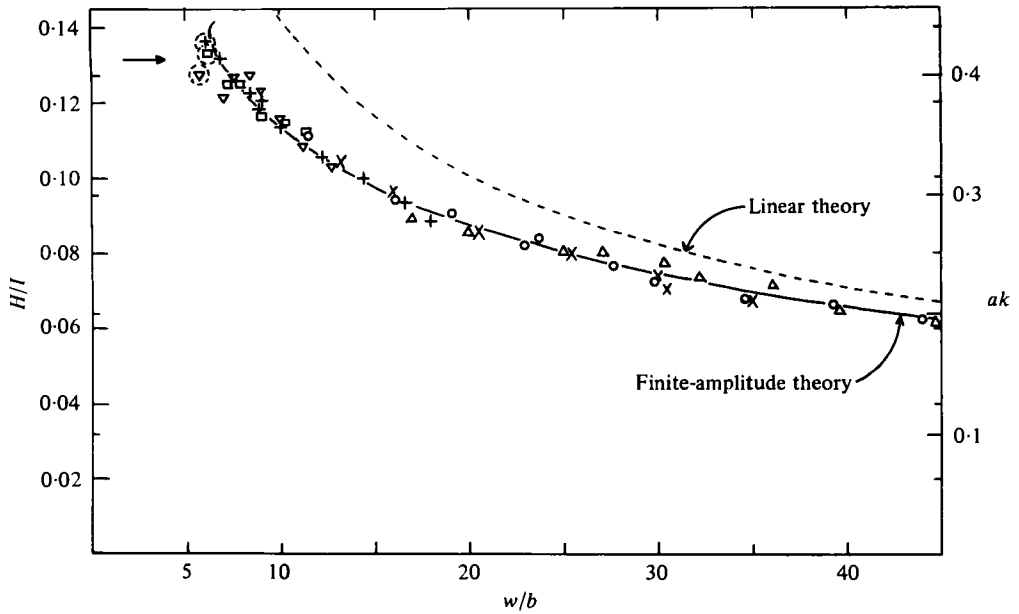


FIGURE 4. A comparison of theory and van Dorn & Pazan's (1975) experimental results. Measurements of breaking waves are indicated by surrounding the point by a broken circle. The experimental points are *not* being compared with linear theory. The solution for linear theory is included for comparison with the finite-amplitude theory only, please see the text. For 0.66 Hz:  $\circ$ , *A*; +, *B*;  $\square$ , *C*. For 0.73 Hz:  $\triangle$ , *A*;  $\nabla$ , *B*.  $\times$ , 0.80 Hz, *A*.

passes through the centroid of each data set; but there is no intrinsic reason for using any other method of choosing  $b_0$  and  $b_1$ .

To gain a measure of whether the finite-amplitude theory is any better than linear theory one must consider the differences from the theoretical curve. The standard deviation is a measure of dispersion about the mean. The values of the standard deviation of the 'constants'  $b_0$  and  $b_1$  have been calculated for each data set; call them  $\sigma_0$  and  $\sigma_1$ . The values of  $\bar{b}_0$  and  $\bar{b}_1$  differ so much from each other that the quantities  $\sigma_0/\bar{b}_0$  and  $\sigma_1/\bar{b}_1$  should give a better measure of the relative agreement.† These are given in table 1. Examination of the numbers in that table shows that in every case the points have less dispersion for the finite-amplitude theory. For one of the largest data sets, 0.66 Hz experiment *B*, the spread is more than halved. This data set includes the steepest wave measured. It should be noted in considering figure 4 that if the points had been plotted using linear theory they would have clustered about that theoretical line.

In figure 4 breaking waves are indicated by broken circles. In the same region of the figure there is an arrow at the steepness  $ak = 0.41$  or  $H/L = 0.13$ . This is the critical steepness at which Longuet-Higgins (1978) finds that deep-water waves become unstable to a rapidly growing instability. Numerical experiments (Longuet-Higgins & Cokelet 1978) show that the instability leads to wave breaking. There is remarkably

† A straight comparison of  $\sigma_0$  and  $\sigma_1$  gives no advantage to the linear theory except for experiment *B* at 0.66 Hz, which is, however, the set with the largest range of high-steepness waves. Which of  $\sigma_i/\bar{b}_i$  or  $\sigma_i$  is the better for comparison depends on the error structure of the measurements. A brief error analysis indicates that for steep waves the former gives a fairer comparison.

Frequency (Hz)	Expt.	Measured points	$\bar{b}_0$	$\bar{b}_1$	$\sigma_0/\bar{b}_0$	$\sigma_1/\bar{b}_1$
0.66	A	10	3.82	4.88	0.068	0.050
	B	10	7.45	11.54	0.084	0.041
	C	6	11.49	18.84	0.110	0.074
0.73	A	9	3.60	4.45	0.101	0.094
	B	8	9.61	15.81	0.140	0.118
0.80	A	8	3.75	4.89	0.076	0.067

TABLE 1

good agreement between this criterion and the few relevant experimental points. If all of van Dorn & Pazan's (1975) data points are examined, it is seen that the steepest wave they measure has  $ak = 0.43$ . The relevance of this type of solution to wave breaking is discussed at greater length in Stiassnie & Peregrine (1980); however, for finite depth of water analysis corresponding to Longuet-Higgins's (1978) result is not available.

## 5. Radial solutions

There is another simple special solution, which has waves with radial crests. That is,  $\alpha = \frac{1}{2}\pi$ , hence  $b = 0$  and

$$rk = n. \quad (5.1)$$

These are waves such that the phase speed  $c = \sigma/k = \sigma r/n$  is proportional to distance from the origin. All that this requires is that the wave steepness increases appropriately with  $r$ . That is, according to

$$r = gnS/\sigma^2, \quad \text{or} \quad R = S. \quad (5.2)$$

A plot of steepness,  $ak$ , against  $R$  is given in figure 6. The solution only exists for

$$1.0 \leq R < 1.194.$$

The only comparable linear solution is for waves in a circular cylinder where an edge-wave, or whispering-gallery, mode exists. It is found by setting the first maximum of  $J_n(kr)$  at the cylinder's boundary; this determines  $k$  (see figure 3, the cylinder boundary is at  $kr = 11.8$  for  $n = 10$ ). For large  $n$  this maximum is at

$$R \sim 1 + 0.809n^{-\frac{1}{2}} + O(n^{-\frac{3}{2}}), \quad (5.3)$$

which is always less than 1.194 for  $n > 8$ .

## 6. The general case

The behaviour of solutions for the full range of values of  $C$ ,  $0 < C < \infty$ , can be better understood by noting the limiting values. In §4 the case  $C = 0$  is dealt with. As can be seen from the solution and experiments there is a radius at which waves break. For small values of  $C$  similar behaviour can be expected. Perhaps this is most easily seen from ray diagrams scaled such that the radius of breaking is constant as in figure 5.

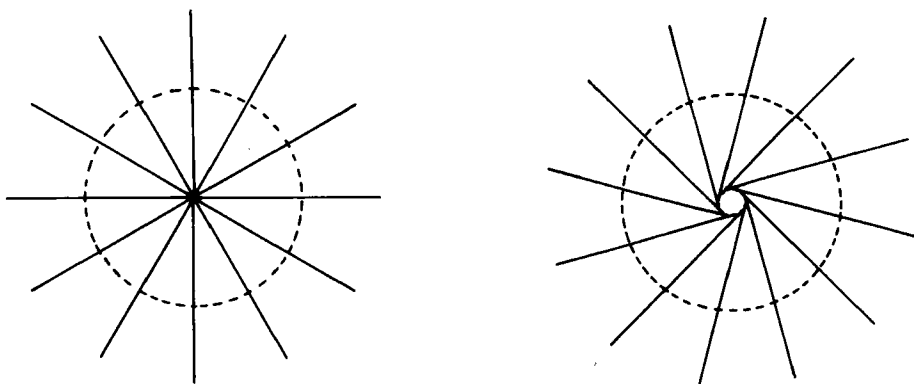


FIGURE 5. Linear-ray diagrams for  $C = 0$  and for  $C$  small, drawn with a constant radius of wave breaking.

Convergence of wave action dominates the wave behaviour and the caustic is too remote to be relevant. From equation (3.4) it can be seen that this behaviour certainly occurs when

$$1 \ll \frac{4\sigma^{16}b^2}{g^8 n^2 [S^8(E + 5L)]_{\max}}. \tag{6.1}$$

That is when

$$C \ll 2/[S^4(E + 5L)]_{\max} \simeq 10. \tag{6.2}$$

For large values of  $C$  there is a non-uniformity. For the case of §5,  $C = \infty$  and we have the radially oriented waves. On the other hand, as  $C \rightarrow \infty$  for fixed  $\sigma$  and  $n$  the wave-action flux approaches zero and the linear solution of §2 is appropriate. As can be seen below, this non-uniformity is reflected in the solutions for large  $C$ , which for a finite range of  $r$  are not unique but have two branches corresponding to the two solutions just mentioned.

It is quite straightforward to calculate solutions for any value of  $C$  using the approximate expressions for  $S(s)$ ,  $E(s)$  and  $L(s)$  given by I, or directly from the tables of Longuet-Higgins (1975) or Cokelet (1977). The dimensionless versions of equations (3.3), (3.4) and (3.5) may be written:

$$K = 1/S, \tag{6.3}$$

$$\tan \alpha = \frac{1}{2}CS^4(E + 5L) \tag{6.4}$$

and

$$R = S \operatorname{cosec} \alpha. \tag{6.5}$$

Figure 6 shows some sample solutions for the steepness,  $ak$ , as a function of  $R$ . The curve for  $C = 20$  is qualitatively little different from that for  $C = 0$  given in figure 4. The next solution, for  $C = 50$ , is different. It has a vertical tangent at a steepness below the 'breaking steepness' and hence a singularity in the approximate solution which may not indicate breaking. There is a second solution branch at higher steepnesses for a very limited range of  $R$ . Higher values of  $C$  show the 'caustic singularity' moving to a more gentle steepness and the second solution becoming more pronounced.

The two solutions for  $C = \infty$ , waves of zero steepness and waves with radial crests, are indicated. These limit the solutions for large  $C$ . On the other hand, the linear ray-theory solution can be applied for non-zero amplitude. It is

$$K = 1, \quad \sin \alpha = R^{-1}, \quad s = a^2 k^2 = 4/CR \cos \alpha, \tag{6.6}, (6.7), (6.8)}$$

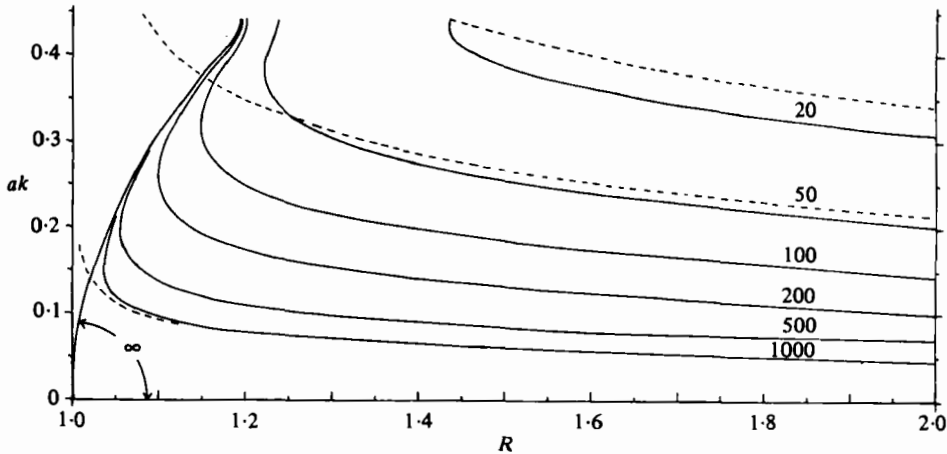


FIGURE 6. Steepness as a function of  $R$  for waves approaching a circular caustic. The numbers indicate the value of the caustic parameter,  $C$ , on each curve. Full lines are finite-amplitude solutions, broken lines are linear ray-theory solutions.

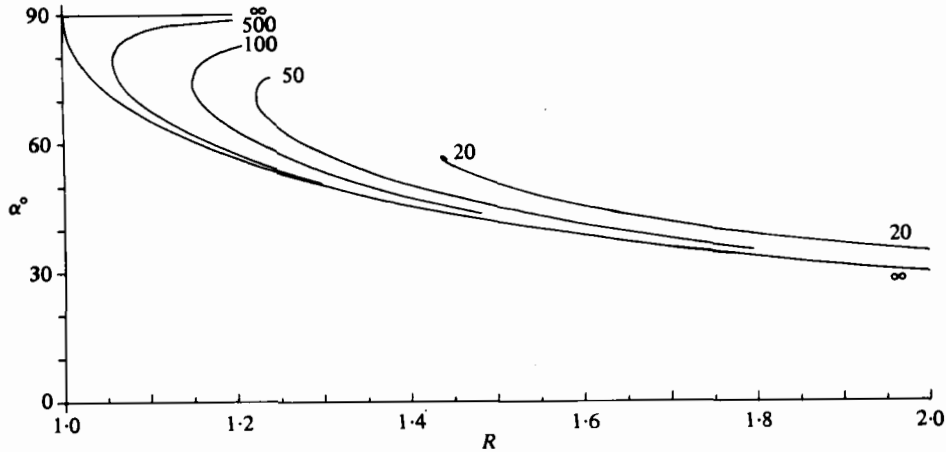


FIGURE 7. The angle,  $\alpha$ , between the wavenumber vector and the radius vector as a function of  $R$  for waves approaching a circular caustic. The numbers indicate the value of the caustic parameter,  $C$ , on each curve.

in our dimensionless variables. Three examples are indicated in figure 6 by broken lines. The finite-amplitude solution for  $C = 1000$  is so close to the linear solution until its singularity that one can expect the linear theory, especially the exact solution, to be superior for such large values of  $C$ .

The direction of wave propagation for finite-amplitude waves deviates from that of linear waves, as is clear from comparison of equations (6.5) and (6.7). This deviation may be seen in the solutions for  $\alpha(R)$  given in figure 7. The variation of  $\alpha$  for linear waves corresponds to straight-line propagation and is the lower solution for  $C = \infty$  in the figure. The two solutions for  $C = \infty$  can again be seen to limit the two branches of the solution for large values of  $C$ . The direction of deviation from a straight line for the finite-amplitude waves is away from the region of steeper waves.

## 7. Conclusions

The study of the refraction of finite-amplitude water waves is carried further in two important respects. The comparison with experiment shown in figure 4 and table 1 indicates that this approach can be more accurate than linear theory and that, in conjunction with Longuet-Higgins's (1978) theoretical result, it is successful in predicting the occurrence of wave breaking. Secondly, as foreshadowed by the general results for the 'modulation velocities' of nonlinear waves, the solutions presented in §5 demonstrate quite explicitly that propagation along 'rays' derived from linear theory is inadequate for nonlinear waves. If lines everywhere parallel with the wave-number vector are considered, these are curved in these examples even though the medium is uniform.

It is rarely that refraction of water waves propagating on deep still water is of any importance, but when it is  $C$  can be estimated from (3.9) and linear theory. For finite water depths, Stiassnie & Peregrine (1980) compare solutions for waves normally incident on a beach with experiments. The comparison is less convincing than figure 4 since waves in finite depth of water suffer more dissipation and there are more likely to be other disturbing effects due to mean flows. The behaviour of finite-depth, finite-amplitude waves near a caustic is likely to be similar to that of deep-water waves. Ryrie & Peregrine (1981) show that no new features arise at a straight caustic caused directly by variation of the depth. Further work is needed to confirm the expectation that circular caustics in constant water depth are similar to those described here.

All the finite-amplitude solutions omit interaction with reflected waves. This is satisfactory for the case of a perfect focus (§3) and other cases where the caustic parameter  $C$  is less than about 20 since the theory predicts that waves break. In which case they may be expected to dissipate much of their energy in the process. For the larger values of  $C$ , especially  $C > 50$ , the solutions suggest that waves do not break and presumably are reflected. Near-linear theory can deal with these cases, see Peregrine & Smith (1979), and work is in progress to examine this further. However, at present there seems to be no prospect of dealing with this aspect for truly finite-amplitude waves.

The work described in §3 was presented at the European Mechanics Colloquium, 102, 'Breaking waves; surf and run up on beaches' at the University of Bristol, 18–21 July 1978.

## REFERENCES

- ABRAMOWITZ, M. & STEGUN, I. A. 1964 *Handbook of Mathematical Functions*. Washington: National Bureau of Standards.
- COKELET, E. D. 1977 Steep gravity waves in water of arbitrary uniform depth. *Phil. Trans. Roy. Soc. A* **286**, 183–230.
- CRAPPER, G. D. 1979 Energy and momentum integrals for progressive capillary-gravity waves. *J. Fluid Mech.* **94**, 13–24.
- HAYES, W. D. 1973 Group velocity and nonlinear dispersive wave propagation. *Proc. Roy. Soc. A* **332**, 199–221.
- LONGUET-HIGGINS, M. S. 1975 Integral properties of periodic gravity waves of finite amplitude. *Proc. Roy. Soc. A* **342**, 157–174.
- LONGUET-HIGGINS, M. S. 1978 The instabilities of gravity waves of finite amplitude in deep water. II. Subharmonics. *Proc. Roy. Soc. A* **360**, 489–505.

- LONGUET-HIGGINS, M. S. & COKELET, E. D. 1978 The deformation of steep surface waves on water. II. Growth of normal mode instabilities. *Proc. Roy. Soc. A* **364**, 1-28.
- PEREGRINE, D. H. & SMITH, R. 1979 Nonlinear effects upon waves near caustics. *Phil. Trans. Roy. Soc. A* **292**, 341-370.
- PEREGRINE, D. H. & THOMAS, G. P. 1979 Finite-amplitude deep-water waves on currents. *Phil. Trans. Roy. Soc. A* **292**, 371-390.
- PHILLIPS, O. M. 1966 *The Dynamics of the Upper Ocean*. Cambridge University Press.
- RYRIE, S. & PEREGRINE, D. H. 1981 Refraction of finite-amplitude water waves obliquely incident to a uniform beach. (Submitted for publication.)
- STIASSNIE, M. & PEREGRINE, D. H. 1979 On averaged equations for finite-amplitude water waves. *J. Fluid Mech.* **94**, 401-405.
- STIASSNIE, M. & PEREGRINE, D. H. 1980 Shoaling of finite-amplitude surface waves on water of slowly-varying depth. *J. Fluid Mech.* **97**, 783-805.
- VAN DORN, W. G. & PAZAN, S. E. 1975 Laboratory investigation of wave breaking, Part II: Deep water waves. *A.O.E.L. Rep.* no. 71, SIO Ref. no. 75-21. Scripps Institution of Oceanog., Univ. of Calif. San Diego.
- WHITHAM, G. B. 1974 *Linear and Non-Linear Waves*. Wiley-Interscience.